Romanian Journal of Ophthalmology, Volume 60, Issue 2, April-June 2016. pp:79-89

GENERAL ARTICLE

Diagnosis of non-exudative (DRY) age related macular degeneration by non-invasive photon-correlation spectroscopy

Fankhauser Franz II* *, Ott Maria**, Munteanu Mihnea*****
***Augen Zentrum Fankhauser AG, Bern, Switzerland**
****Martin-Luther-Universität Halle-Wittenberg, Germany**
*****Department of Ophthalmology, "Victor Babes" University of Medicine and Pharmacology, Timisoara, Romania**

Correspondence to: Franz Fankhauser II, MD,
Augen Zentrum Fankhauser AG, Bern, Switzerland,
Gutenbergstrasse 18, 3012 Bern, Switzerland.
Phone: +41 (0)31 301 9880, Fax: +41 (0)31 301 9881,
E-mail: franz.fankhauser@augenzentrum-fankhauser.ch

Accepted: April 25, 2016

Abstract

Purpose. Photon-correlation spectroscopy (PCS) (quasi-elastic light scattering spectroscopy, dynamic light scattering spectroscopy) allows the non-invasively reveal of local dynamics and local heterogeneities of macromolecular systems. The capability of this technique to diagnose the retinal pathologies by in-vivo investigations of spatial anomalies of retinas displaying non-exudative senile macular degeneration was evaluated. Further, the potential use of the technique for the diagnosis of the macular degeneration was analyzed and displayed by the Receiver Operating Curve (ROC).

Methods. The maculae and the peripheral retina of 73 normal eyes and of 26 eyes afflicted by an early stage of non-exudative senile macular degeneration were characterized by time-correlation functions and analyzed in terms of characteristic decay times and apparent size distributions.

Results. The characteristics of the obtained time-correlation functions of the eyes afflicted with nonexudative macular degeneration and of normal eyes differed significantly, which could be referred to a significant change of the nano- and microstructure of the investigated pathologic maculas.

Conclusions. Photon-correlation spectroscopy is able to assess the macromolecular and microstructural aberrations in the macula afflicted by non-exudative, senile macular degeneration. It has been demonstrated that macromolecules of this disease show a characteristic abnormal behavior in the macula.

Keywords: photon-correlation spectroscopy, quasi-elastic light scattering spectroscopy, dynamic light scattering spectroscopy, non-exudative (dry) age related macular degeneration

Introduction

Photon-correlation spectroscopy (PCS) has been known for more than 50 years. Today it has become a standard technique for detecting random thermal movements to reveal sizes and

shapes together with the diffusion constants of suspended particles, such as macromolecules in gels and in other complex liquid systems [1-7]. In ophthalmology, PCS has been performed in the cornea, the aqueous humour and the vitreous. Such examinations have been performed under physiologic as well as in pathologic conditions [8-13]. It has been shown that it is possible to determine the dimensions of such particles in the range of about 1-1000 nm. PCS seems to be very appropriate for the application in ophthalmology because it is non-invasive and it can make biochemical processes visible both at the microscopic, macromolecular and supramolecular level. Pathologic processes can be observed both directly, in real time and under optimal conditions in the living tissues. When we assume that most pathologic processes are already present as molecular or macromolecular alterations during a certain period before, the disease actually starts. Hence, it would be very advantageous to establish easy-accessible and non-invasive diagnostic tools, which are able to reliably detect such molecular preclinical pathology before the disease actually begins, perhaps at a time when therapy is more effective.

Subjects

PCS measurements were performed on 73 eyes (of 84 normal patients) and 26 eyes (of 26 patients suffering from non-exudative, senile macular degeneration [NESMD]) (see Table 1).

Table 1. Demography of the normal and abnormal subjects tested

	Normals	Nonexudative age-related macular degeneration
Total number of eyes	73	20
Average age (years)	60.5	65.5
Average visual acuity	0.9	0.6
Worst visual acuity	0.9	0.3
Best visual acuity	1.1	0.8
Central fixation	+	+
Other pathology	-	-
Neovascular vessels by fluorescein angiography	-	-

The average age of the normal patients was 60.5 years and for the abnormal patients 65.5 years. The experiments were performed with the written consent of the subjects and under the oversight of the local ethics committee of the University of Dresden, Germany. The Declaration of Helsinki on human rights was complied with. Both the normals and the abnormals were scheduled for cataract surgery following the experiments.

The average visual acuities for the normals were 0.8 (least: 0.5) and for the abnormals 0.7 (least 0.4). A routined specialist with a Goldmann 3-mirror contact lens studied the eyes; the only disease accepted being a non-exudative, dry, senile, macular degeneration. The criteria were soft or hard drusen [14,15].

Method

The diagnostic laser beam was emitted from a HeNe laser, working at 632.8 nm, and was operated at 1.5 to 15 μW. These values were well below the safety limits (55 μW during 20 minutes) stipulated by the American National Standards Institute (ANSI) Z-136 for the safe use of lasers, New York. The pupils were dilated with Diopine 10 and local anesthesia was induced by 0.4% Novesine. The focal spot was set at the macula by a hollow-beam aiming system [16] (Fig. 1a,1b).

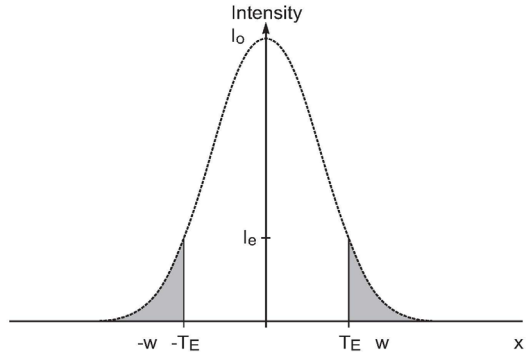

Fig. 1a Distribution of laser light intensity, which originally had a Gaussian shape and a maximum intensity Io. I_e is the maximum intensity of the beam that was used and Ti and w are the inside and outside radii, respectively, of the hollow beam

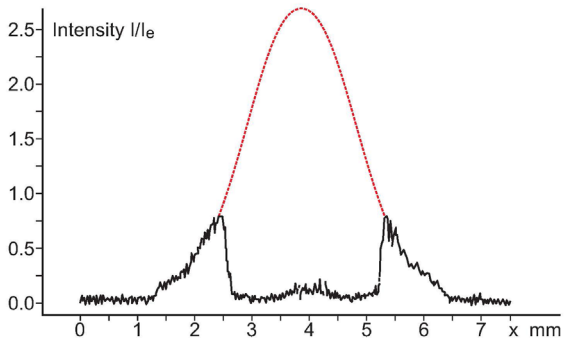

Fig. 1b Square shape of the hollow beam at a plane perpendicular to the beam's propagation

Hence, when the focus is anterior or posterior to the macula or retina, a ring occurs, but when the focus coincides with the macula, one spot is seen, as observed with the microscope of the instrument. The ellipsoid-shaped focal volume (640 μm^3 in air) had the lateral dimensions of 2.5x2.5 μm^2 and the axial dimension of 84 µm.

During the operation, an auxiliary fixation spot is shown to the patient and three locations are determined: C1 (center), C2 (6° temporal) and C3 (12° temporal) (Fig. 2).

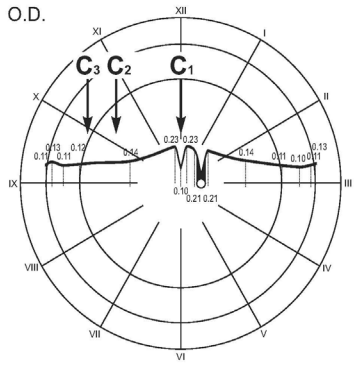

Fig. 2 Optical section through a human retina. The figures are thicknesses of the retina and C1, C2 and C3 are the test locations

One measurement of an intensity correlation function took on average about 10 seconds. One measurement cycle consisted of 5 measurements, which were average. The correlation functions were observed on-line on a monitor and, when abnormalities of the curves were seen, e.g. induced by eye movements during the measurements, the curves were discarded and the measurement repeated. The criterion for a "good" correlation curve is a stable plateau not disturbed by noise at the beginning, a steep decay and a flat final plateau at y=1.

In addition, the measurements were constantly verified by a computer program in respect to noise in the optical and electric system [**17**].

The intensity of the diagnostic stray light was measured by an avalanche diode (EG&G, SPCM-AQ-WX1-FZ, Vaudreil, Canada), which was correlated with a digital correlator AL-5000, 5.0, ALV Germany). It contains a single photon counting diode (SPAD) fed by a stabilized high voltage supply. For the wavelength used (632.8 nm), the quantum efficiency of our avalanche diode exceeded that of a photomultiplier by a factor of about 4 and was therefore well adapted for the weak stray light signals emitted by an eye [**18**]. The dead time of the electronics was 30 ns and did not interfere with the measurements because the correlation time of one measurement was approximately 1 ms.

The measurements were performed in the lower linear range of the photodetector, i.e., between 20 and 100 Hz. Here the correction for the dead time is between 0.99 and 1.01. At 20 Hz, the background corresponds to 1.7% and, at 100 Hz, to 0.4% of the measured counting rate. The digital signal was correlated and symmetrically normalized by means of multiple schemes [**19**]. This kind of symmetrization optimizes the statistical accuracy for long delay times. It has to be noted, that only the intensity auto-correlation function $g^{(2)}(\tau)$ can be measured, which for comparative and quantitative analysis needs to be transformed into the electric field autocorrelation $g^{(1)}(\tau)$ function by Eq. 7. Only the field auto-correlation will be discussed in the article, which for simplicity will be called auto-correlation function only.

Results

The location of the center and the peripheral are defined as 0° and 12° temporal with respect to the macula (see C1 and C3 in **Fig. 2**). The auto-correlation functions of the investigated eyes

usually showed a characteristic decay of around 1 ms, whereas the decay time obtained for the macula (C1) in the absence of NESMD consistently showed a longer characteristic decay compared to both peripheral measurements (C2, C3). Hence, a parameter Δg was defined as the difference of the correlation functions at the relaxation time of 1 ms. It was found that this definition of Δg is very robust and can be reliably used to discern between pathological and normal eyes. **Fig. 3** shows a typical set of auto-correlation curves obtained at the center (macula) and at the periphery of a normal 50-year-old subject. **Fig. 4** compares typical auto-correlation functions of an eye with and without NESMD. The eye with NESMD has a Δg of about zero, since the auto-correlation functions of the center typically coincide with the peripheral measurement. It should be noted that the peripheral auto-correlation functions are similar to those for the normal case.

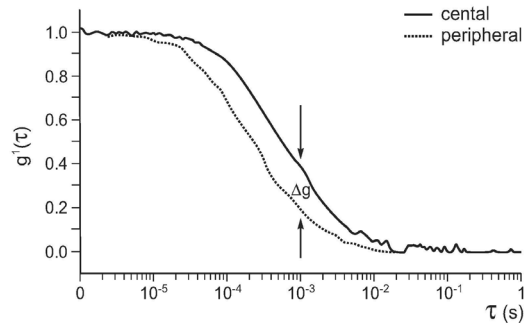

Fig. 3 Electric field correlation function $g^{(1)}_{(\tau)}$ at the center and the periphery of a normal subject of 50 years. Δg is the difference of the correlation curves at a delay time τ of 1 ms

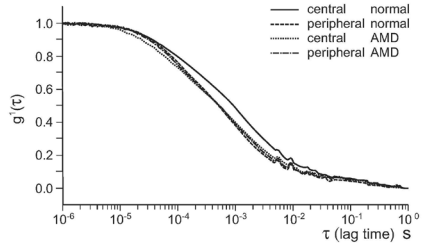

Fig. 4 Comparison of the electric field correlation functions at the degenerated macula C1; the normal macula -C1 and the normal periphery C3

Next to this rather fast analysis, in which the typical decays are compared, one can also analyze the most probable size distributions of the scatterers. These distributions can be obtained from the auto-correlation functions by regularization methods (see **Appendix**) and display the apparent sizes distribution as expected for spherical scatters in a homogeneous solution. In respect to the viscosity, local heterogeneities, local interactions, or shape will lead to an apparent broadening of the obtained distribution. **Fig. 5** compares the apparent size distributions obtained by averaging over all the measurements taken at the macula of the normal and pathologic cases and by assuming a constant viscosity of η = 1.16. As expected, a shift to smaller sizes can be discovered.

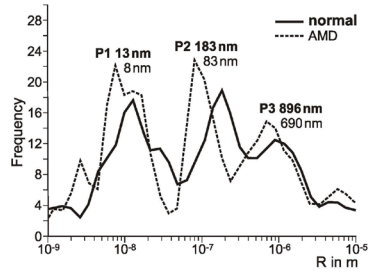

Fig. 5 Change of distribution of apparent sizes of particles and diffusion coefficients in the normal and diseased macula

Following this, a frequency distribution of the differences of the auto-correlation functions at the center and at the periphery was computed by averaging two measurements at each test location (**Fig. 6**).

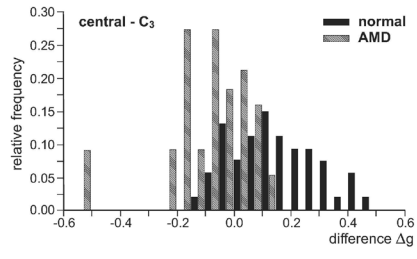

Fig. 6 Distribution of relative frequencies of the differences of the electric field auto-correlation functions at the center vs. the periphery for the normal and an abnormal eye. The width of the intervals is 0.1

The determinations of Δg were performed at 1 ms and at the widths of the intervals was 0.1. Negative differences refer to the cases in which the auto-correlation curves taken at the center are below the peripheral auto-correlation curve. It was found that in 46% of the normal eyes, Δg is always greater than Δg in the abnormal (NESMD) eye. In eyes with NESMD 45% of the Δg, differences were smaller than -0.1. In order to discriminate normals from abnormals a threshold value is required; i.e., when the differences are greater than this threshold, the eye is normal and the diagnosis is negative (no disease). When this is not the case, the diagnosis is positive; i.e., there is disease. At a threshold of 0.05, the values in the convergence table (**Table 3**) were obtained. From this table it results that the sensitivities at a threshold of 0.05 are 78%, whereas the selectivity is 72%.

These data are displayed by a ROC curve (receiver operating curve) [**20**] in **Fig. 7**. The quality of a test is given by a large area below the ROC, which means that the curve stays close to x=0.0 for low values (highly selective) while quickly approaching y=1.0 (highly sensitive).

Table 2. Radii and diffusion constants (from **Fig. 5**)

Radius (nm)	Diffusion constant (m^2/ s)
8	2.5×10^{-11}
10	2.0×10^{-11}
13	1.5×10^{-11}
83	2.4×10^{-12}
183	1.1×10^{-12}
690	2.8×10^{-12}
896	2.2×10^{-12}

Table 3. Convergence table for the measurements performed, provided their differences between central and peripheral correlation function at τ = 1 ms with Δg > 0.05 being normal and those with Δg < 0.05 being abnormal

Retina condition	Diagnostic result		Total
	Positive	Negative	
AMD	0.78	0.22	1.0
no AMD	0.28	0.72	1.0

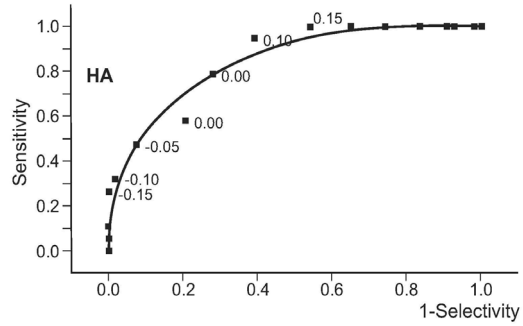

Fig. 7 ROC curve for the diagnosis of NESMD, realized by the differences of the auto-correlation curves $g^{(1)}_{(\tau)}$, measured at the macula and the peripheral retina at τ = 1. The values, computed with the help of **Table 2**, are displayed as black squares. The adjacent figures are the threshold values. The black line is the fit-function

It also follows that the more false diagnoses are accepted, the more the probability of a correct diagnosis rises. It is clear from the ROC curve that Δg =0.00 corresponds to the value in which one measurement deviates most from the correlation curve. However, since for each test location only two measurements were available, one can assume that a better averaging would approach the correlation curve better. The area under the ROC curve is the average of the selectivity of all the sensitivity values.

Discussion

Photon correlation spectroscopy is a non-invasive optical method that is able to monitor the translational mobility of molecules or small mobile particles in colloidal solutions and ocular tissues. The investigations of this study at the retina showed that PCS has even the capability to differentiate *in-vivo* between normals as compared to those with NESMD. In polydispersed, biological tissues, such as in this case, it measures an assembly of various molecular identities. The identification is non-trivial, as for a more extensive analysis of the individual entities of the scatterers, the auto-correlation functions must eventually be inverted (Eq. 6), which leads to an ill-poised mathematical problem, the result being disturbed by noise. It is for this reason that the

determination of the microparticles displays some amount of noise interaction [**19**]. Despite such limitations, the size determinations have been shown to be possible [**4-13**].

This clinical study was performed on 73 normal eyes and on 20 eyes afflicted with NESMD. The measurements (i.e., the determinations of the autocorrelation functions) were performed at the macula and at two selected extra-macular retinal sites. The temporal correlations of the fluctuations of the scattered light were then computed and the molecular sizes were derived from them. For this, the electrical field must be deduced from the intensity measurements of the stray light.

Despite the individual differences of the correlations, the apparent size distributions of the particles at the various retinal locations could be measured and compared. In normal eyes, the autocorrelation functions obtained at the center and at various peripheral retinal sites differ. When the eyes with NESMD were compared, such differences vanished and the sizes of the scatterers in the macular region were shifted to lower values. This led to the conclusion that the differences between the fovea (macula) and the periphery are caused by an alteration of the stray light characteristics of the foveal cones. Since the strongly scattering properties of melanin also add to the measured signal, degenerative alterations of the pigment epithelium and perhaps its lack may also cause this abnormal stray light behavior.

Both an abnormal stray light behavior of the receptors, of the pigment epithelium, and of other microparticles of the retina may work together. We have found macromolecular size distributions at about 15, 80, and 900 nm.

However, if the diagnosis of a macular disease by simple means is aimed at, only one (repeated) measurement at the macula and one at a peripheral site would be required and an inversion of the correlation function is not necessary.

In summary, the differences of central versus peripheral stray light behavior were quantified and these were then analyzed by a ROC (receiver operating curve) function that was able to correctly diagnose this disease at a given probability, here at a sensitivity of 78% and a selectivity of 72%. An overlap of the difference values of the auto-correlation functions of normals as compared to abnormal was found. The reason for this may be the fact that the leading bioindicator for the disease was an anatomical criterion, i.e., most of the time the criterion being "hard or soft drusen" [**14,15**]. While drusen are an important indicator for the NESMD, normally functioning areas may have still existed in these maculae, while in maculae, termed "normal" pathological areas may have existed already. It is important to know that the average sensitivity of all sensitivities is 0.85. It lies in a range where other diagnostic methods in medicine are also found [**20**].

Various approaches are available for an improvement of the accuracy of the photon correlation spectroscopy at the retina. These are methods related to data collection and analysis but also methods related to an improvement of the measuring system. The accuracy of the data collection procedure can be improved by increasing the number of measurements at one location, because at various retinal regions, the average values differ only slightly. The determination of the autocorrelation function could be increased by a suitable filter function. Here we have characterized the correlation functions via measurements of time. Perhaps the other parameters, such as the measurement of the area under the autocorrelation function (curve) may increase the accuracy. Most importantly: an optimization of the determination of the particle size distribution should be intensified. Here, also an introduction of dedicated filter functions, the development of a stray light model of the retina, the automatic detection of data, which are affected by eye motions, appear important. Just as important are the local determinations of the refractive indices and viscosities. This would lead to an optimization of the determination of the sizes of the particles.

Also, a better understanding of these distribution functions would improve the sensitivity and the specificity of the inversion procedure. This could lead to a better understanding of the mechanism of the central and peripheral stray light behavior and this could increase the diagnostic power. Further, the measuring system could be improved and better adapted to the specific conditions of the retina. It should be noted that with the present apparatus, stray particles that are larger than the wavelength of the exiting laser beam could indeed be detected, but the detected radii are somewhat smaller than the true ones. When a source with a longer wavelength is used instead

of HeNe laser light (632.8 nm), the measurements of the particles would be improved. According to the spectral properties (absorption) of the eye, the wavelengths of 900 and 110 nm would be well suited. Here, another advantage would be to increase the maximal exposure duration/ energy (BGI 2003). This would result in an augmented signal/ noise ratio. This would be important when measuring cataract eyes, in which a laser power of 30 μW at a wavelength of 632.8 nm is often not enough. The measuring inaccuracy and the disturbing effect of eye movements could be partly or totally inhibited by measuring the central and peripheral retinal sites simultaneously.

Appendix

Theory of photon correlation spectroscopy

When light interacts with material, scattering particles alter the direction of its propagation [**21**]. The angle distribution of the scattered light – with respect to the incoming light beam – depends thereby on the sizes and positions of the scatterers. Hence, the scattered light carries detailed information on the molecules or microstructures from which it is scattered. The information of the scatterers is encoded in temporal intensity fluctuations I(t) of the scattered laser light and can be analyzed by calculating the autocorrelation function of the detected light intensity $g^2(\tau)$:

$$g^2(\tau) = 1 + \frac{\langle I(t)I(t+\tau)\rangle}{\left(\langle I\rangle\tau\right)^2} \qquad \text{Eq. 1}$$

Thereby, intensity fluctuations mainly originate from the motions of the particles with respect to each other. Furthermore, the rotational movements of non-spherical particles or changes in the observed volume will also lead to fluctuations.

The random movements of unbound particles can be described by the mathematical model of Brownian motion, which characterizes the motions by a translational diffusion coefficient D.

This diffusion coefficient gives access to the sizes of the scatterers, since it inversely depends on the hydrodynamic radius (R_h) of the particle as given by the Stokes-Einstein equation:

$$D = \frac{k_B T}{6\pi\eta R_h} \qquad \text{Eq. 2}$$

where η corresponds to the viscosity of the surrounding solvent, T is the temperature, and k_B is the Bolzmann constant.

Relatively small particles with large diffusion coefficients show fast molecular movements which lead to only briefly correlated fluctuations of the scattered light.

To characterize the decay of the correlation function it is helpful to define a relaxation rate Γ (or decay constant τ_c) by

$$\Gamma = \frac{1}{\tau_c} = q^2 D \qquad \text{Eq. 3}$$

which also accounts for the spatial distribution of the scattered intensity described by the scattering vector q:

$$q = \frac{4\pi n}{\lambda}\sin(\theta/2) \qquad \text{Eq. 4}$$

for a scattering angle of θ

For monodisperse solutions, the relaxation rate is linked to the autocorrelation function $g^2(\tau)$ by

$$g^{(2)}(\tau) = I_0\left(1 + \exp\{-2\Gamma\tau\}\right) \qquad \text{Eq.5}$$

In case of a polydispersed solution $g^{(2)}(\tau)$, the determination of the distribution of $G(\Gamma)$ becomes an ill-posed problem and has to be derived from the correlation function of the electric field, $g^{(1)}(\tau)$.

Provided there is no interaction by parasitic, static stray light and there is no particle-particle interactions, the electric field correlation function $g^{(1)}(\tau)$ and the measured intensity correlation function $g^{(2)}(\tau)$ are related by Siegert's relation:

$$g^{(2)}(\tau) = 1 + |g^{(1)}(\tau)|^2 \qquad \text{Eq. 6}$$

The size distribution of the particles yields the intensity autocorrelation function $g^{(2)}(\tau)$, which consists of superimposed exponential functions with decay times corresponding to the r distribution. Polynomial fit procedures have been described before [**22**].

$$g^{(1)}(\tau) = \int_0^\infty G(\Gamma)\exp(-\Gamma\tau)d\Gamma \qquad \text{Eq.7}$$

G (Γ) must be analyzed by CONTIN regularization program [**23**].

Heterodyning

Two correlation functions should be discriminated, i.e. the correlation function of the light intensity $g^{(2)}(\tau)$ and the correlation function which measures the electric field $g^{(1)}(\tau)$. One can measure light intensity but not the electric field. Hence, the two quantities must be correlated by means of Eq. 9. Principally speaking, two possibilities for such a correlation exist. The first is the homodyne method. Here the intensity of the scattered light is measured and its correlation function is determined. In the other, the heterodyne version, the diagnostic HeNe laser light is split into two. One of the beams is directed to the sample. The resulting backscattered light is then superimposed with the non-scattered light and directed to the detector.

This same effect is seen when, under non-ideal conditions, the heterodyne portion is superimposed upon the diagnostic (homodyne) beam. This is called partial heterodyning [**24**], falsifying the information in the autocorrelation function. This effect is observed in non-ideal conditions such as in-situ experiments in the eye. Here, unpleasant side effects may occur and one has to expect interferences of unknown amounts of parasitic stray light. Such stray light may be generated, for instance, at the surface of a contact lens but also, e.g. by collagenous fiber strands or membranes in proliferative, diabetic vitreo-retinopathy. The case of weak heterodyning is very problematic in the sense that merely a small decrease of the amplitude of the correlation function (= the coherence factor) is observed while the more important distortion of the correlation function may be lost from sight. For example, with a 45% local oscillator, the amplitude decreases by only 15% but the error in the estimation of the hydrodynamic radius of a particle is 40%.

For purely homodyne experiments, the Siegert relation is the following:

$$g^{(2)}(\tau) = 1 + \beta \mid g^{(1)}(\tau) \mid^2 \qquad \text{Eq. 9}$$

β is the coherence factor 0 < β <1. In monomode fibers, such as the ones used here, β is 1. It decreases when parasitic stray light (e.g. an incoherent background light) intrudes into the measuring system, but also when e.g. dead-light or saturation effects of the detector are observed. This is what could happen (to a larger or smaller extent) in the eye. Such global noise effects can be detected e.g., by the program of Flammer and Ricka [**22**]. Due to heterodyning, Eq. 9 is no longer valid and the heterodyne parameter h must be introduced:

$$h = I_l / I_s \qquad \text{Eq. 10}$$

where I_l is the homodyne (diagnostic) signal and I_s the heterodyne (parasitic) light. Now Eq. 9 must be corrected and replaced by:

$$g^2(\tau) = 1 + \frac{h}{(1+h)^2}\,\mathrm{Re}\left\{g^{(1)}(\tau)\right\} + \frac{h}{(1+h)^2}\,\mathrm{Re}\left|g^{(1)}(\tau)\right|^2$$

Eq. 11

where the parameter h can be obtained from Eq. 12:

$$h = \frac{1}{g^{(2)}(0) - 1} - 1 \qquad \text{Eq. 12}$$

We are now in the position to compute $g^{(1)}(\tau)$ from $g^{(2)}(\tau)$ and can perform an analysis of our data.

Apparatus

Because of space limitations due to the pupil size, the optical system used has the excitation beam (into the eye) and the beam carrying the scattered light (out of the eye) in common. This system has been used before [18] and is described elsewhere [18]. Hence, we shall restrict ourselves to some key elements.

Radiation Source

The radiation source used for these experiments is a HeNe laser (Uniphase 1103P, California, USA) working at a power of 20 mW. The emitted wavelength is 638.2 nm, 20% of which is absorbed on its way to the retina. The wavelength used is also from a range that is least toxic for the receptors because, according to Planck's law, photon energy decreases with wavelength increase. Therefore, the retinal metabolism is the least disturbed. A monomode optical fiber (TEM-mode > 95%) is used for light conduction, being coupled into the system by a coupler. In contrast with multimode fibers, monomode fibers have the advantage that higher modes are suppressed and that the exciting beam has a Gaussian profile.

Optical Diagram

The Gaussian intensity distribution of the exciting beam is:

$$I(x) = I_0 e^{-2 (x-x_0) / w^2} \quad \text{Eq.13}$$

where w is the distance at which the maximum intensity at the x_0 has fallen to e^{-2} (= 13.5%) of the maximum. A Haag-Streit slit-lamp (900BQ) is part of the apparatus. In addition, various optical supplementary parts were shown to be necessary for these experiments (Fig. 1b,8,9) and had to be supplemented. The laser beam was given a hollow intensity distribution (Fig. 8). In this, the excitation and diagnostic beams pass through the same optical elements (Fig. 8). In this optical system, the focal planes of the observation, diagnostic and excitation beams are the same. Hence, an exact localization of these beams during the experiment is possible. In Fig. 8, the principle ray paths during one measurement at the retina are shown. The red beam is the excitation beam and the blue one is the measurement, i.e. the scattered, diagnostic beam. Instead of using all possible scattering angles for computations, the scattering angle, an average scattering angle = 6° corresponds to an angle of 4.5° in water and to 4.1° in the retina (n=1.35). The scattering angle is $\theta = 180° - \alpha_s$. For this situation a correlation time $\tau_c = 0.31 \pm 0.15$ ms can be computed for latex spheres (100 nm diameter) for 100 nm = 0.3 ms when a constant scattering vector is used. For all the possible scattering vectors, a correction of only 0.1% would be required. From this, it follows that for high precision, a constant angle of θ_s suffices for a precise description of the light scattering.

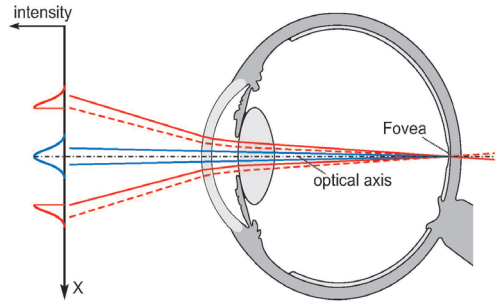

Fig. 8 Schematic optical scheme. The hollow beam (red) is used for focusing. Blue part of the stray light beam reaching the detector

Intensity Distribution in the Focus and in the Scattering Volume

We are interested in the intensity distribution of the hollow beam and its focus (Fig. 9), the focal depth and the scattering volume. Taking advantage of Huygen-Fresnel's principle, the intensity distribution near the focus, as shown in Fig. 8, is obtained. The integrals to be computed were solved numerically by MATHEMATICA 4.0 program. When the focus of the excitation beam is at the retina, it corresponds to a numerical aperture of 15 mm for a pupil diameter of 6 mm. Fig. 8 displays the intensity distribution along the optical axis and in the radial direction. The isoline used for both the excitation and the scattered volumes is the place intensity has decreased to 50% of the maximal value.

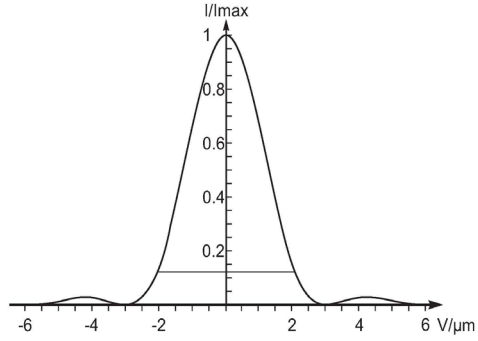

Fig. 9 Intensity distribution perpendicular to the focal plane

Scattering Beam

The focal volume V of the exciting beam is stimulated by its electric field. This is given by an overlapping integral of the stimulating and the scattering beam.

$$V = \int dr\, I_e(r)\, I_s(r) \qquad \text{Eq.14}$$

In air, this volume amounts to 640 m^3. The isoline at which the intensity has decreased to 50% of the maximum is an ellipsoid having a width of 2.5 μm and a length of 84 μm in air. At the retina this amounts (n=1.35) to a width of 3.4 μm and to a length of 154 μm. The resulting resolution suffices to have at least 2 photoreceptors in the focal volume. The focal length of 154 μm also suffices to have both the receptor layer and the pigment epithelial in focus simultaneously.

Limitations of the Laser Power

In order to avoid thermal and photochemical damage to the retina by high laser power, the excitation power of the laser beam is decreased by a thermal filter. Damage to the retina depends both on the duration and on the power of the laser beam. According to the specifications of ANSI Z 1361 (1993), a maximal laser power of 55 μW (measured at the cornea) and an irradiation duration of 20 minutes avoids damage. The laser power was measured before each examination with a Silica detector. In addition, a maximum laser power was used in order to adjust the counting rate of the detector. In patients with reasonably clear lenses, an examination could usually be performed with 20 μW. When the opacity of the lens was considerable, not even 30 μW were able to generate a signal.

Detector and correlator

The intensity of the stray light was measured with a single–photon counting module (SPAD), having a high voltage, voltage-stabilized supply. The quantum efficiency for the wavelength is better than 4 times that of a photomultipler and is therefore ideally suited for registering the weak stray light signals of the retina. Because the autocorrelation time of the retina has an order of magnitude of 1 ms, the dead time of 1μs therefore suffices to measure the decay constant. The measurements were performed in the lower range of the photon detector, i.e. between 20 kHz and 100 kHz. In this case, the correction for the dead time is of 0.99 and 1.01. The amount of the background radiation corresponds, at a frequency of 20 kHz, to 1.7% and, at 100 kHz, to 0.4% of the counting rate. The digital measuring signals were correlated by means of a Tau scheme [19] and were symmetrically normalized. This kind of symmetrization optimizes the statistical accuracy, particularly for measurements with large delay times. Two monitor channels, one for the direct and one for the delayed counting rates, were used. The product of the average values of the direct and the retarded channels [19] is used for normalization. By a display of the autocorrelation curves during the measurements on the screens, these could be evaluated already during the measurements and hence could be repeated, if necessary. The criterion of a "good" autocorrelation curve is when a stable initial plateau, undisturbed by noise, contains a steep slope and a final plateau at y=1.

Eye movements

Three types of involuntary eye movements exist: (i) drifts, (ii) microsaccades, (iii) microtremor. Drifts are the slowest movements, having amplitudes of 2.5 angular minutes and a speed of 2 to 8 angular minutes per second. Microsaccades have amplitudes of 3 to 50 angular minutes and a linear maximal velocity that depends on the amplitude of the motion. Microtremor, which is a kind of correcting movement, has an amplitude of less than 12 angular minutes, a velocity of 10 angular minutes per second, and a frequency of about 30 Hz.

The diffusion constant of spherical particles is indirectly proportional to its hydrodynamic radius. Hence, in order to assess the influence of involuntary eye movements, the moved retina can be treated as a static particle for which diffusion constants and the hydrodynamic radii can be computed. Consequently, the above-mentioned drifts can be compared with the apparent movements of the static particles that lie between 1x10-11 m/ second and 5x10-11 m/ second. The apparent movements of the static particles are therefore 1 to 2 orders of magnitude higher than the diffusion constant of a 100 nm diameter particle. According to the Stokes-Einstein relationship, the apparent diffusion constants of the eye drifts correspond to hydrodynamic radii between 5 and 20 nm. As a result, the static particles that are apparently moved by eye drifts would be assigned hydrodynamic radii of 5 to 20 nm and microsaccades and microtremors would

yield values of 5 nm and 20 nm, respectively. Hence, disturbances due to involuntary eye movements are negligible. However, slow movements due to voluntary movements can be highly disturbing and should be suppressed as far as possible. The Goldmann contact lens is helpful in this respect, because it inhibits eye movements. Negative suction contact lenses would inhibit eye motions altogether.

Acknowledgements

This work was supported by Haag-Streit International. The author had full access to all the data in the study and takes responsibility for the integrity of the data and the accuracy of the data analysis. The authors gratefully acknowledge the editorial assistance of Arthur Funkhouser. The explanations of characteristic features of nonexudative (dry) macular degeneration by Hans E. Grossniklaus have been greatly appreciated.

References

1. Fankhauser F II. Dynamic light scattering in ophthalmology. Results of in vitro and in vivo experiments. Technol Health Care. 2006; 14(6):521-35.
2. Berne B, Pecora R. Dynamic Light Scattering. 1985, New York, Plenum Press.
3. Brown. Dynamic Dynamic Light Scattering. 1993, Oxford, Clarendon Press.
4. Chu B. Laser Light Scattering. 1974, New York, Academic Press.
5. Chu B. Laser Light Scattering. Basic Principles and Practice, 1991, Boston, Academic Press.
6. Chu B. Selected papers on quasi-elastic elastic light scattering by macromolecular, supramolecular and fluid systems. 1990, Bellingham, The International Society for Optical Engineering.
7. Schmitz KS. Dynamic Light Scattering by Macromolecules. 1990, San Diego, Academic Press.
8. Bursell SE, Serur JF, Haughton H, Nipper JN, Sinclair JR, Spears JR, Paulin S. Cholesterol levels assessed with photon correlation spectroscopy. Proc SPIE. 1986; 712:175-182.
9. Cummins HZ, Pike ER. Photon Correlation and Light Beating Spectroscopy, 1974, New York, Plenum Press.
10. Farrell RA, Bargeron CB, Green WR, McCally. Collaborative biomedical research on corneal structure. Johns Hopkins APL Techn Digest 4. 1983; 65-79.
11. Hart RW, Farrell RA. Light Scattering in the cornea. J Opt Soc Am. 1969; 59:766-774.
12. Jedzhiniak JA, Nicoli DF, Baram H, Benedek GB. Quantitative verification of the existence of high molecular weight protein aggregates in the intact normal human lens by light-scattering spectroscopy. Invest Ophthalmol Vis Sci. 1978; 17:51-57.
13. Latina M, Chylack P, Fragerhom P, Nishio I, Tanaka T, Palmquist BM. Dynamic light scattering in the intact rabbit lens. Invest Ophthalmol Vis Sci. 1987; 28:175-183.
14. Green WR, McDonnel PH, Yeo JH. Pathologic features of senile macular degeneration. Ophthalmology. 1985; 92:615-627.
15. Green WR, Enger C. Age-related macular degeneration. Histological studies. The 1992 Lorenz Zimmermann Lecture. Ophthalmology. 1993; 100:15-39.
16. Rovati L, Fankhauser II, Ricka J. Design and performance of a new ophthalmic instrument for dynamic light-scattering measurements in the human eye. Rev Sci Instr. 1996; 67:2615-2620.
17. Flammer I, Ricka J. Dynamic light scattering with single mode receivers: partial heterodyning regime. Appl Opt. 1997; 36:7508-7517.
18. Daulet H, Deschamp P, Dians B, Mc Gregor A et al. Photon counting techniques with silicon avalanche photodiodes. Appl Opt. 1983; 32:3894-3900.
19. Schätzel K. Noise in photon correlation data. I. autocorrelation functions Quantum Opt. 1990; 2:287-305.
20. Zou XH, Obuchowski NA, McClish DK. Statistical Methods in Diagnostic Medicine. 2002, New York, Wiley, 15-56.
21. Cummins HZ, Knable, Yeh Y. Observation of diffusion broadening of Rayleigh scattered light. Phys Rev Lett. 1964; 12:150-153.
22. Koppel DE. Analysis of macromolecular polydispersity in intensity correlation spectroscopy: The method of cumulants. J Chem Phys. 1972; 57(11):4814-4821.
23. Provencher SW. CONTIN: a general purpose constrained regularization program for inverting noisy linear algebraic and integral equations. Comp Phys Comm. 1982; 27:229- 242.
24. Siegert AJF. Radiation Laboratory Report 465, 1943.